

## SUPPLEMENTARY MATERIAL:

### An experimental and kinetic modelling study of *n*-C<sub>4</sub>-C<sub>6</sub> aldehydes oxidation in a jet-stirred reactor.

<sup>1</sup>Matteo Pelucchi\*, <sup>2</sup>Sylvain Namysl, <sup>1</sup>Eliseo Ranzi, <sup>1</sup>Alessio Frassoldati, <sup>2</sup>Olivier Herbinet, <sup>2</sup>Frédérique Battin-Leclerc, <sup>1</sup>Tiziano Faravelli

<sup>1</sup>CRECK Modeling Lab, Department of Chemistry, Materials and Chemical Engineering “G. Natta”, Politecnico di Milano, P.zza Leonardo da Vinci 32, 20133 Milano, Italy

<sup>2</sup> Laboratoire Réactions et Génie des Procédés, CNRS, Université de Lorraine, ENSIC, Nancy Cedex, France

\*Corresponding author: Dr. Matteo Pelucchi, Dipartimento di Chimica, Materiali e Ing. Chimica “G. Natta”, Politecnico di Milano, P.zza Leonardo da Vinci 32, 20133 Milano, Italy.

## 1. Results

This Section presents additional comparisons of experimental measurements carried out in this study with model results.

### 1.1 *n*-butanal

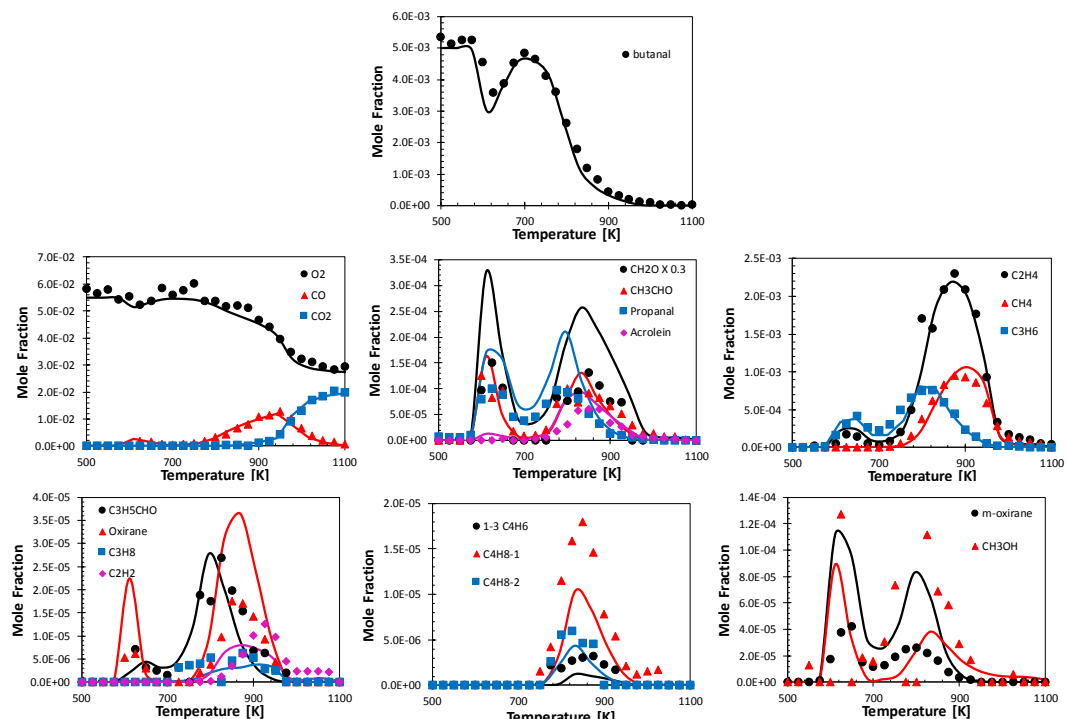


Figure S 1: *n*-butanal/O<sub>2</sub>/He oxidation in a JSR at 1 atm,  $\tau = 2.0$  s, and  $\varphi = 0.5$ . The initial fuel ( $C_3H_7CHO$ ) mole fraction is 0.5%. Symbols: experimental data from this study, lines: model results.

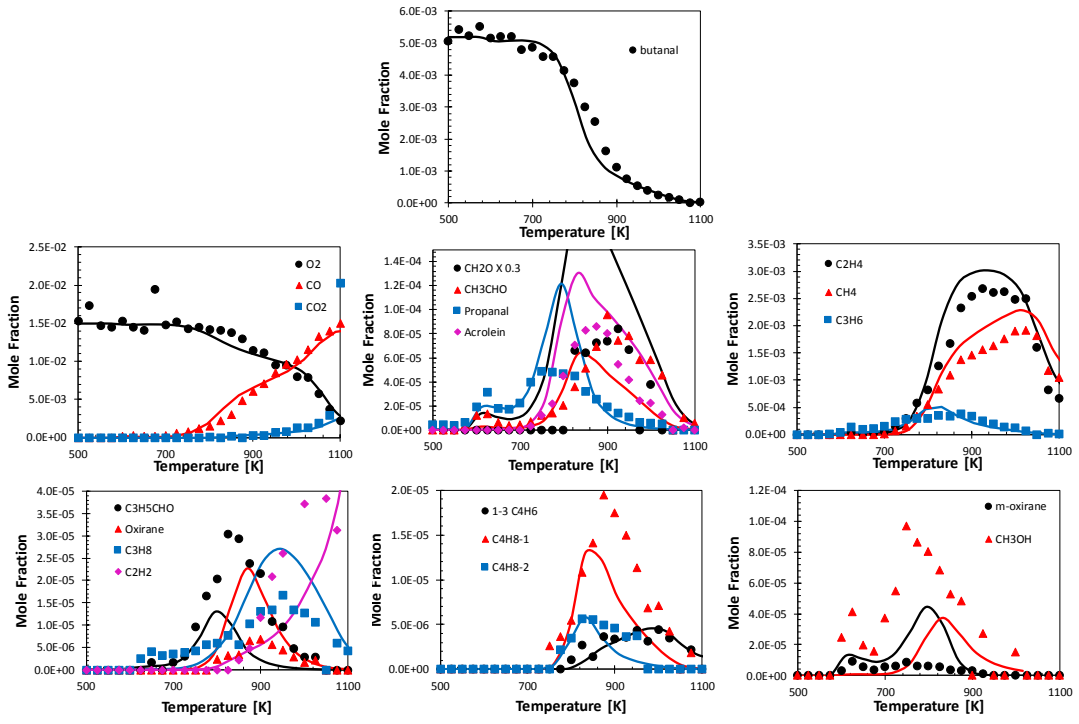


Figure S 2: *n*-butanal/O<sub>2</sub>/He oxidation in a JSR at 1 atm,  $\tau = 2.0$  s, and  $\varphi = 2.0$ . The initial fuel (C<sub>3</sub>H<sub>7</sub>CHO) mole fraction is 0.5%. Symbols: experimental data from this study, lines: model results.

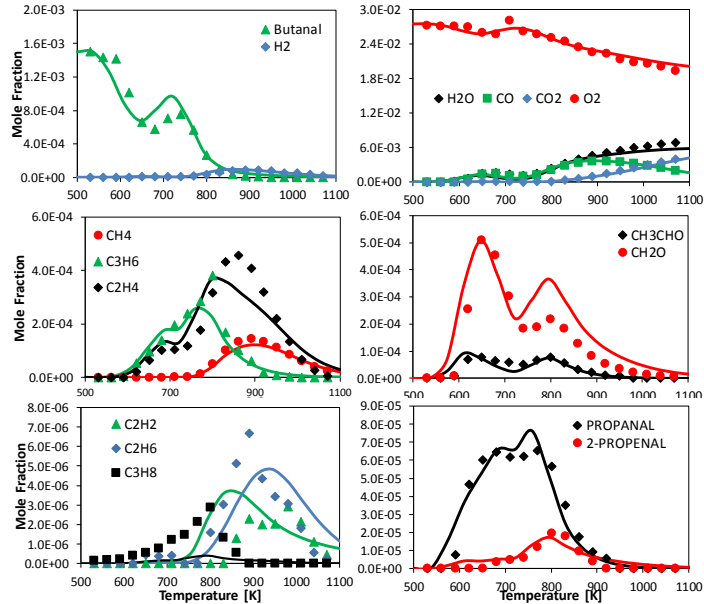


Figure S 3: *n*-butanal/O<sub>2</sub>/N<sub>2</sub> oxidation in a JSR at 10 atm,  $\tau = 0.7$  s, and  $\varphi = 0.3$ . The initial fuel (C<sub>3</sub>H<sub>7</sub>CHO) mole fraction is 0.15%. Symbols: experimental data from Veloo et al., lines: model results.

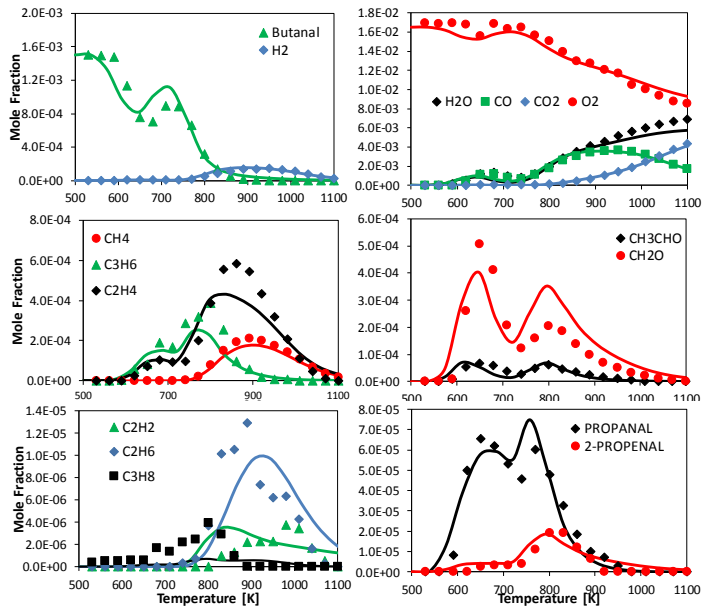


Figure S 4: *n*-butanal/O<sub>2</sub>/N<sub>2</sub> oxidation in a JSR at 10 atm,  $\tau = 0.7$  s, and  $\varphi = 0.5$ . The initial fuel ( $C_3H_7CHO$ ) mole fraction is 0.15%. Symbols: experimental data from Veloo et al., lines: model results.

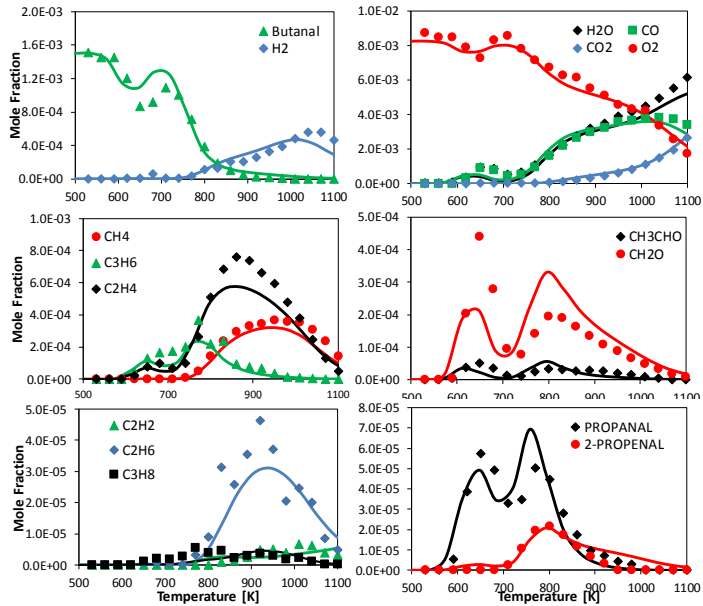


Figure S 5: *n*-butanal/O<sub>2</sub>/N<sub>2</sub> oxidation in a JSR at 10 atm,  $\tau = 0.7$  s, and  $\varphi = 1.0$ . The initial fuel ( $C_3H_7CHO$ ) mole fraction is 0.15%. Symbols: experimental data from Veloo et al., lines: model results.

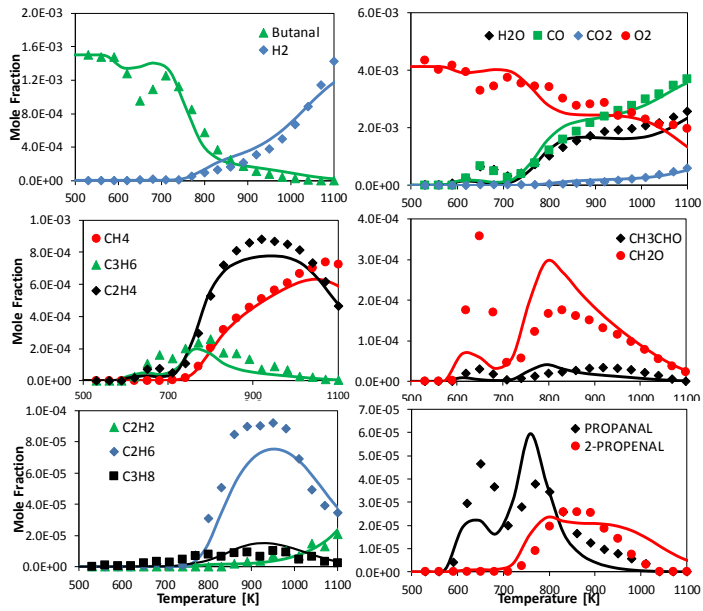


Figure S 6: *n*-butanal/O<sub>2</sub>/N<sub>2</sub> oxidation in a JSR at 10 atm,  $\tau = 0.7$  s, and  $\varphi = 2.0$ . The initial fuel ( $C_3H_7CHO$ ) mole fraction is 0.15%. Symbols: experimental data from Veloo et al., lines: model results.

## 1.2 *n*-pentanal

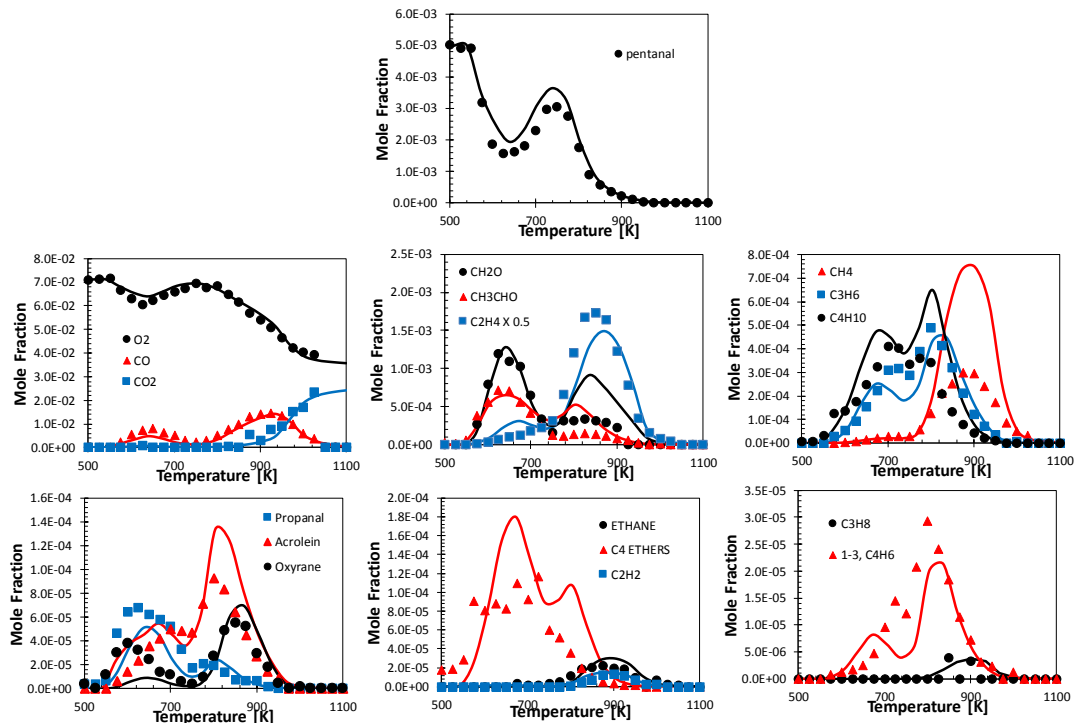


Figure S 7: *n*-pentanal/O<sub>2</sub>/He oxidation in a JSR at 1 atm,  $\tau = 2.0$  s, and  $\varphi = 0.5$ . The initial fuel ( $C_4H_9CHO$ ) mole fraction is 0.5%. Symbols: experimental data from this study, lines: model results.

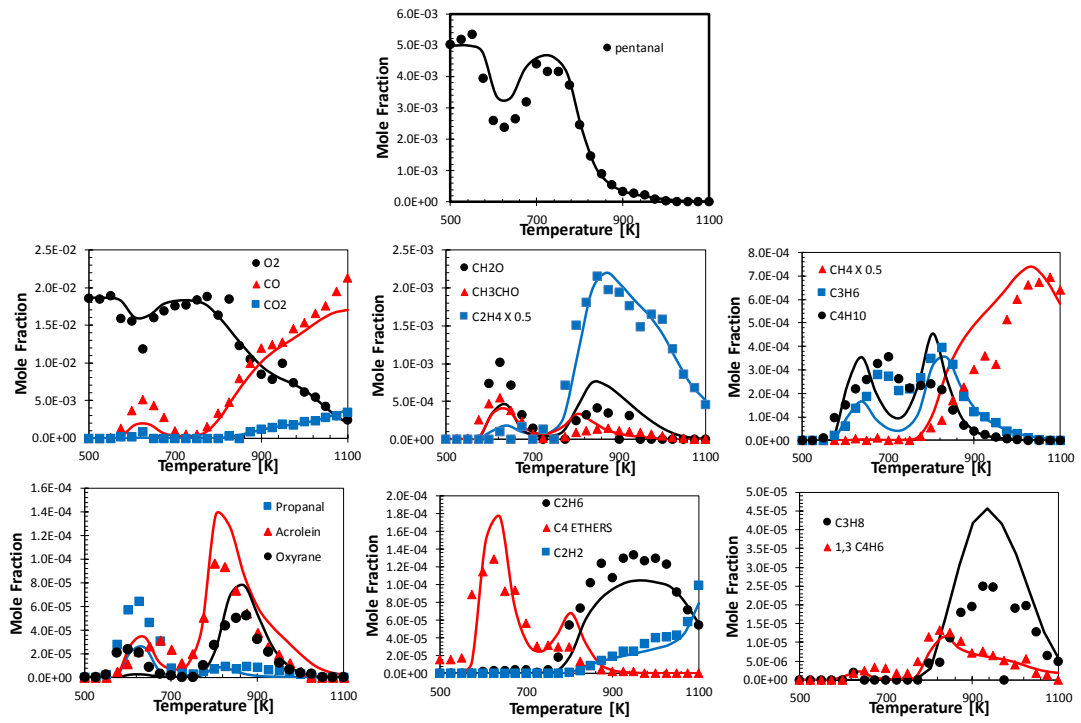


Figure S 8: *n*-pentanal/O<sub>2</sub>/He oxidation in a JSR at 1 atm,  $\tau = 2.0$  s, and  $\varphi = 2.0$ . The initial fuel ( $C_4H_9CHO$ ) mole fraction is 0.5%. Symbols: experimental data from this study, lines: model results.

### 1.3 n-hexanal

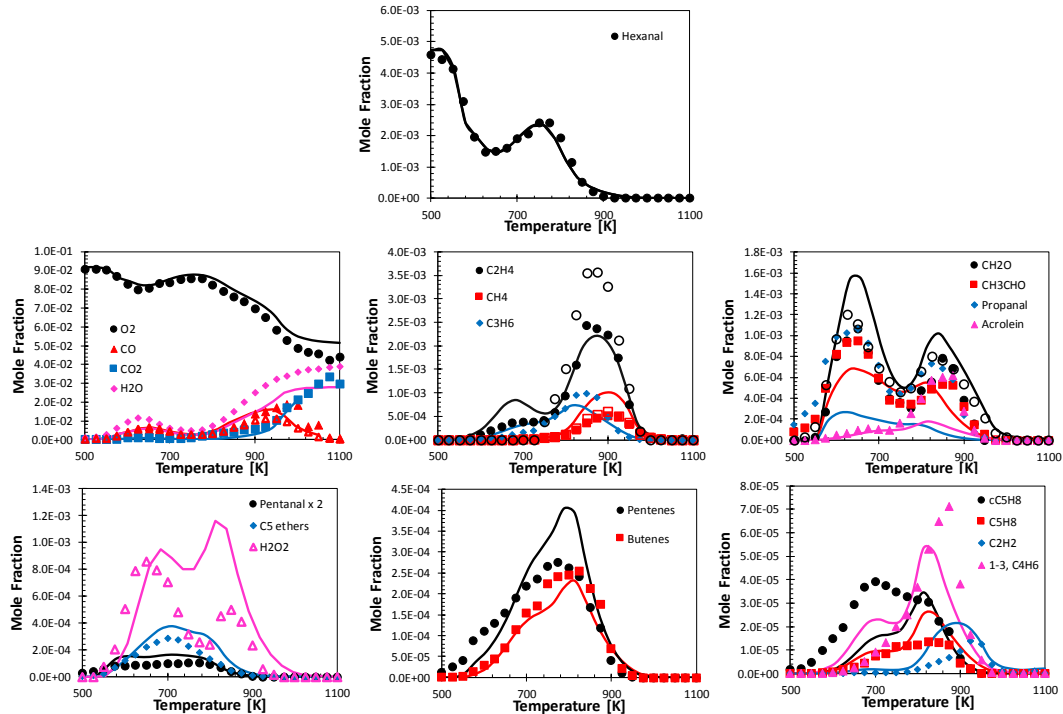


Figure S 9: n-hexanal/O<sub>2</sub>/He oxidation in a JSR at 1 atm,  $\tau = 2.0$  s, and  $\varphi = 0.5$ . The initial fuel (ALDC6) mole fraction is 0.5%. Symbols: experimental data from this study, lines: model results.

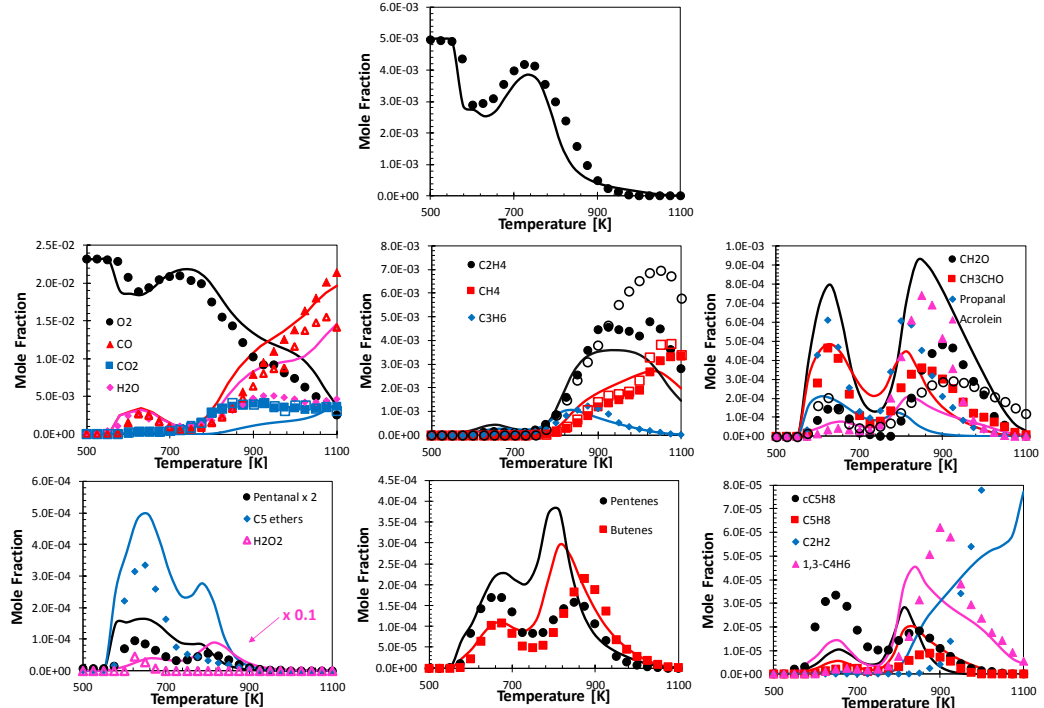
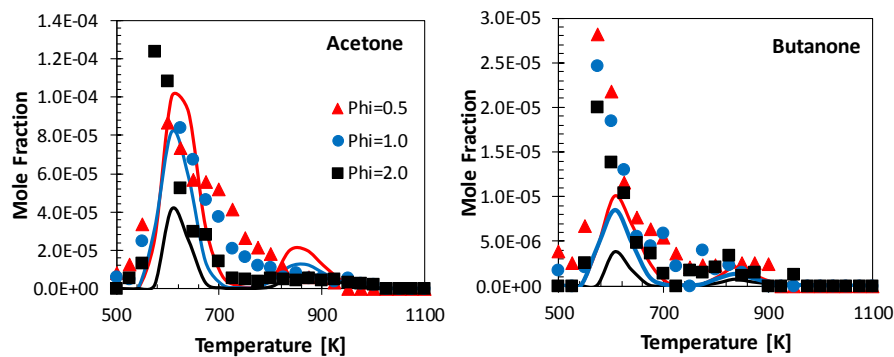


Figure S 10: n-hexanal/O<sub>2</sub>/He oxidation in a JSR at 1 atm,  $\tau = 2.0$  s, and  $\varphi = 2.0$ . The initial fuel (ALDC6) mole fraction is 0.5%. Symbols: experimental data from this study, lines: model results.

## Additional comparisons



*Figure S 11: Acetone and butanone formation in n-pentanal oxidation. Symbols: experimental data from this study, lines: model predictions.*

The decomposition of butane ketohydroperoxides through the Korcek mechanism (*Combust. Flame*, 162 (2015) 1679-1691) explains the low temperature formation of acetone in n-pentanal oxidation. However, formic acid that should be formed together with acetone was not detected.

Butanone formation is explained on the basis of recombination/disproportionation reactions of peroxy radicals butyl radicals, as discussed in Ranzi et al. (*Combust. Flame*, 162 (2015) 1679-1691).

## 2. Lumped Low Temperature Mechanism and Species Nomenclature

*Table S1: Kinetic parameters of the lumped low temperature reactions of n-butanal and n-hexanal.*

Lumped Reactions	n-butanal		n-hexanal	
	A	Ea (cal/mol)	A	Ea (cal/mol)
OH+ALD = H <sub>2</sub> O + CO + R <sub>C<sub>n-1</sub>, alkyl</sub>	2.00E+13	630	2.00E+13	630
OH+ALD = H <sub>2</sub> O + RALD	2.00E+13	1700	3.40E+13	1700
O <sub>2</sub> +RALD => RALDOO	4.00E+12	0	4.00E+12	0
RALDOO => O <sub>2</sub> +RALD	1.00E+13	31500	1.00E+13	31500
RALDOO => QALDX	1.50E+12	25000	3.00E+12	24000
QALDX => RALDOO	3.00E+10	15000	3.00E+10	15000
RALDOO => OH + CO+ C <sub>n-1,aldehyde</sub>	6.00E+11	23500	6.00E+11	23500
RALDOO => CO + C <sub>nalkane</sub> QOOH	3.00E+10	19000	3.00E+10	19000
QALDX => OH + C <sub>n</sub> Lactone	1.00E+12	18000	1.00E+12	17000
QALDX => HO <sub>2</sub> + C <sub>n</sub> Unsat. Ald.	4.00E+13	23500	4.00E+13	23500
QALDX => OH + C <sub>1</sub> Dione + C <sub>m</sub> olefin	2.40E+13	23000	2.40E+13	23000

$\text{QALDX} \Rightarrow \text{OH} + \text{C}_l \text{ Sat. Aldehyde} + \text{C}_m \text{ Unsat. Aldehyde}$	2.40E+13	23000	2.40E+13	23000
$\text{O}_2 + \text{QALDX} \Rightarrow \text{QALDX}$	4.00E+12	0	4.00E+12	0
$\text{ZALDX} \Rightarrow \text{O}_2 + \text{QALDX}$	1.00E+13	31500	1.00E+13	31500
$\text{ZALDX} \Rightarrow \text{OH} + \text{KEALD}$	1.00E+11	18000	1.00E+11	18000
$\text{ZALDX} \Rightarrow \text{OH} + \text{CO} + \text{C}_{n-1,\text{alkane}} \text{ KHYP}$	1.00E+11	18000	1.00E+11	18000
$\text{KEALD} \Rightarrow \text{OH} + \text{Products}$	3.80E+15	41000	3.80E+15	41000

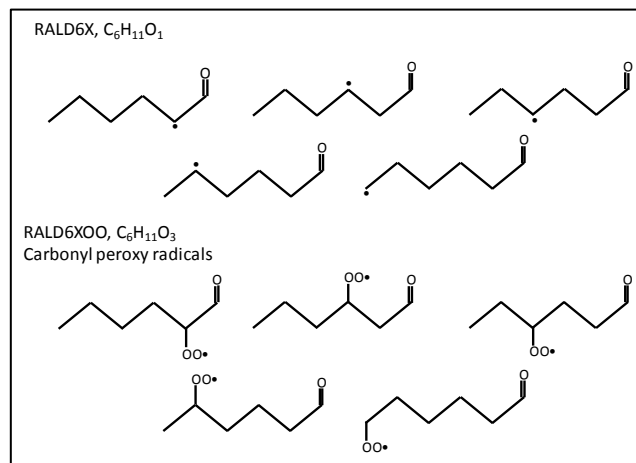


Figure S 12: alkyl radicals (RALD6X) and peroxy carbony radicals (RALD6XOO) from *n*-hexanal (ALDC6) LT oxidation.

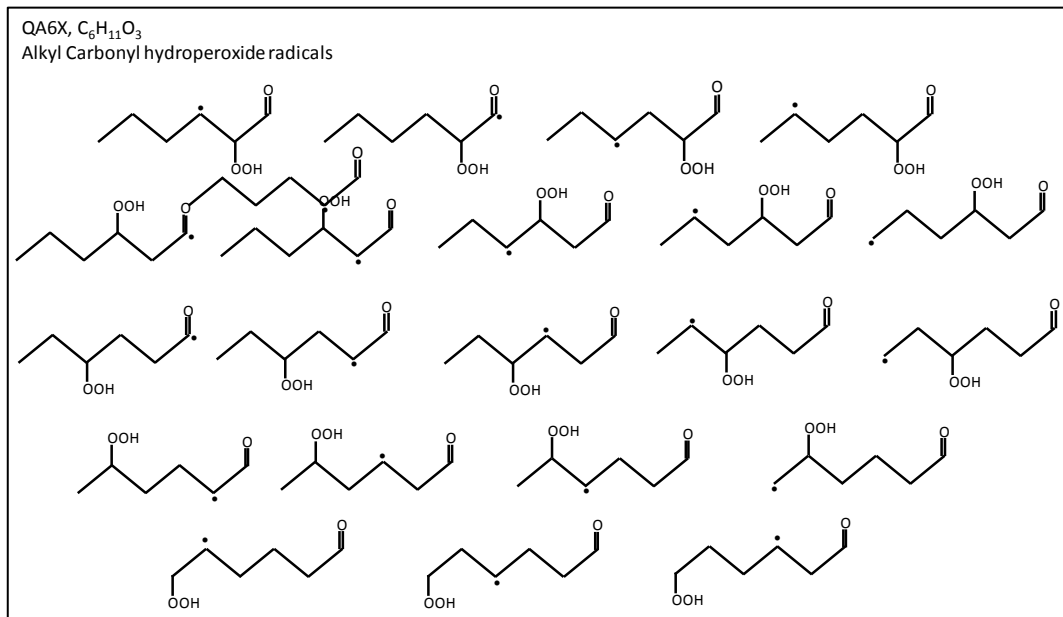


Figure S 13: alkyl carbonyl hydroperoxide radicals (QA6X) from *n*-hexanal LT oxidation.

ZA6X, C<sub>6</sub>H<sub>11</sub>O<sub>5</sub> Peroxy-carbonylhydroperoxide radicals

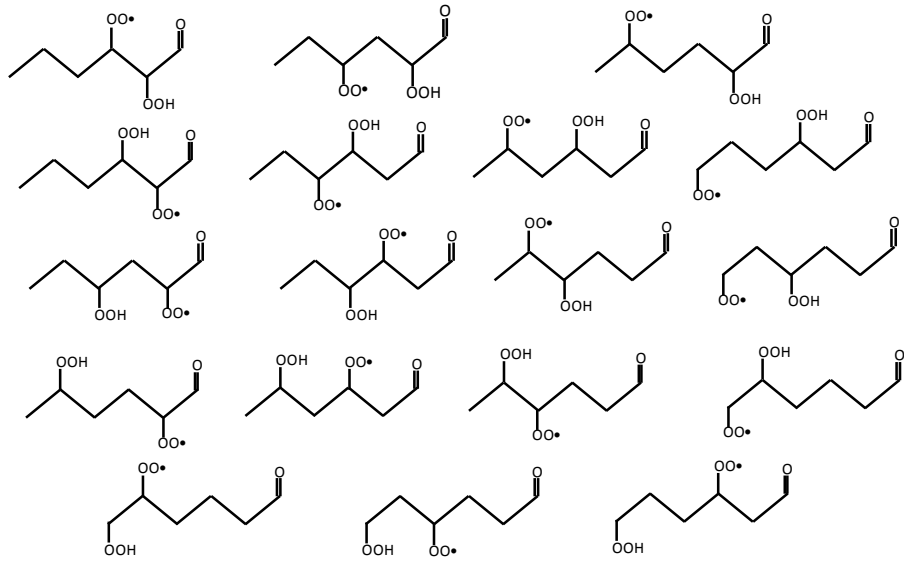


Figure S 14: Figure S 15: Peroxy carbonyl hydroperoxide radicals (ZA6X) from n-hexanal LT oxidation.

KEA6X, C<sub>6</sub>H<sub>10</sub>O<sub>4</sub>  
Di-ketohydroperoxides

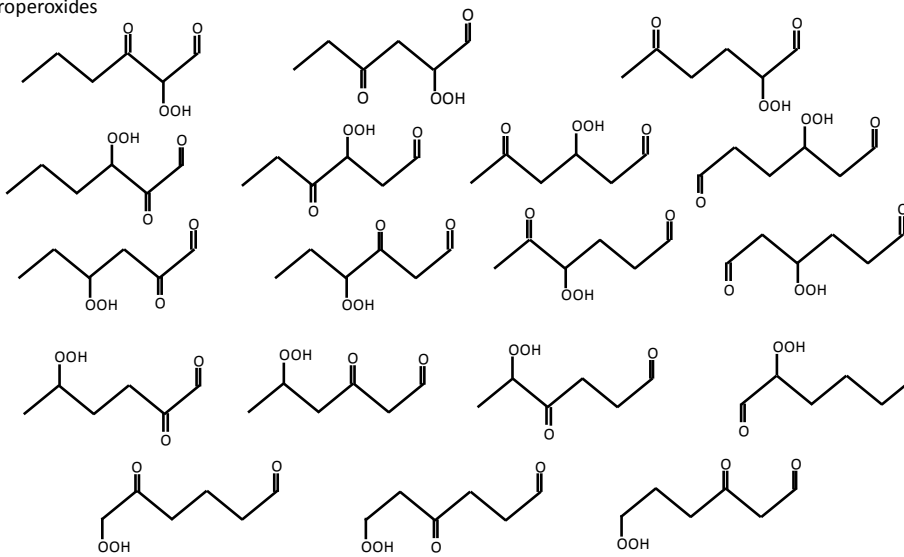


Figure S 16: Di-ketohydroperoxides (KEA6X) from n-hexanal LT oxidation.

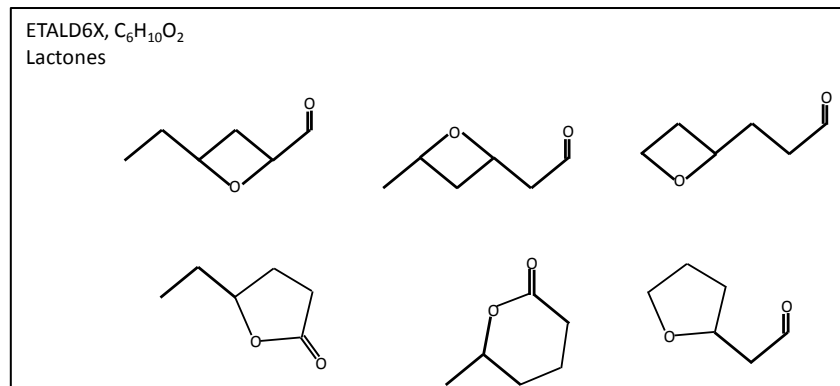


Figure S 17: Lactones (ETALD6X) from n-hexanal LT oxidation.

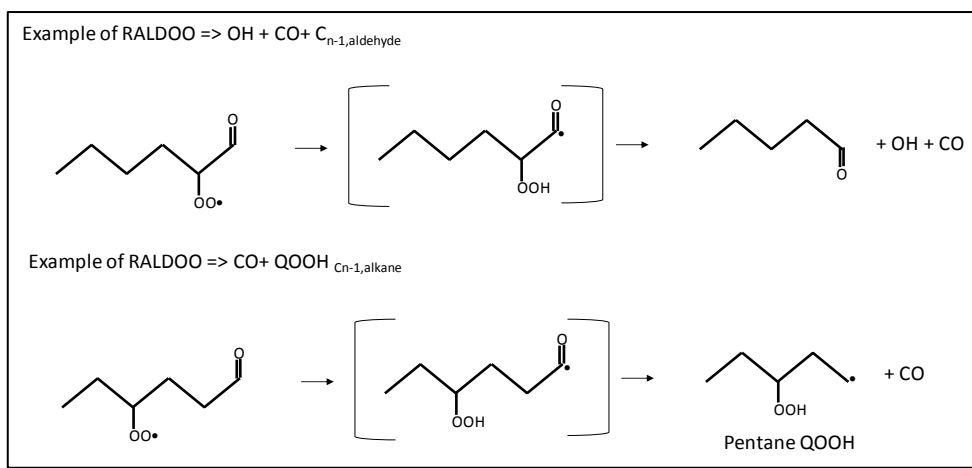
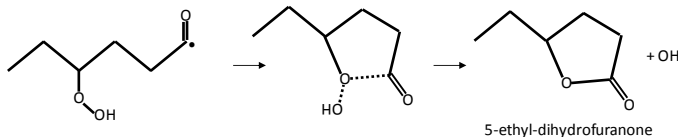
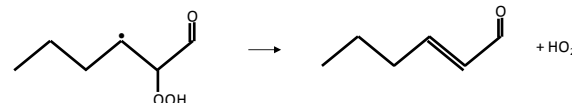


Figure S 18: Example of decomposition reactions of RALD6OOX radical.

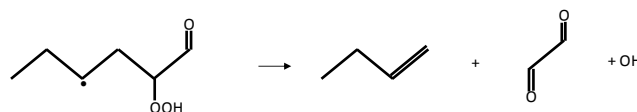
Example of QALDX => OH + Lactone



Example of QALDX => HO<sub>2</sub> + Unsaturated C<sub>n</sub> aldehyde



Example of QALDX => OH + C<sub>l</sub> diones + C<sub>m</sub> alkene ( $l+m=n$ )



Example of QALDX => OH + C<sub>l</sub> Sat. Aldehyde + C<sub>m</sub> Unsat. Aldehyde ( $l+m=n$ )



Figure S 19: Example of decomposition reactions of QA6X radical.

Example of ZALDX => OH + CO+C<sub>n-1,alkane</sub> Ketohydroperoxide

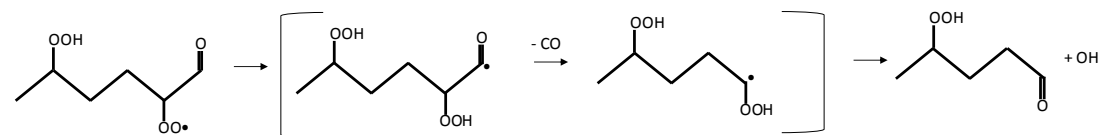


Figure S 20: Example of decomposition reactions of ZA6X radical.

Table S2: nomenclature of other relevant species.

Formula	Name	Nomenclature
<b>n-butanal (C<sub>3</sub>H<sub>7</sub>CHO)</b>		
C <sub>4</sub> H <sub>8</sub> O <sub>3</sub>	Carbonyl peroxy radical	RALD4OOX
C <sub>4</sub> H <sub>8</sub> O <sub>3</sub>	Alkyl Carbonyl hydroperoxide radicals	QA4X
C <sub>4</sub> H <sub>8</sub> O <sub>5</sub>	Peroxy-carbonylhydroperoxide radicals	ZA4X
C <sub>4</sub> H <sub>6</sub> O <sub>4</sub>	Di-ketohydroperoxides	KEA4X
C <sub>4</sub> H <sub>6</sub> O <sub>2</sub>	Butyrolactones	ETALD4X
<b>n-pentanal (C<sub>4</sub>H<sub>9</sub>CHO)</b>		
C <sub>5</sub> H <sub>11</sub> O <sub>2</sub>	Pentyl peroxy radical	NC <sub>5</sub> H <sub>11</sub> -OO
C <sub>5</sub> H <sub>11</sub> O <sub>2</sub>	Pentyl hydroperoxide radical	NC <sub>5</sub> -QOOH
C <sub>5</sub> H <sub>11</sub> O <sub>4</sub>	Peroxy pentyl hydroperoxide radical	NC <sub>5</sub> -OOQOOH
C <sub>5</sub> H <sub>10</sub> O <sub>1</sub>	C <sub>5</sub> cyclic ethers	NC <sub>5</sub> H <sub>10</sub> -O
C <sub>5</sub> H <sub>10</sub> O <sub>3</sub>	Pentane ketohydroperoxide	NC <sub>5</sub> -QOOH
<b>Other species relevant to the LT combustion of n-aldehydes</b>		
C <sub>4</sub> H <sub>6</sub> O <sub>2</sub>	Butanedione	C <sub>4</sub> H <sub>6</sub> O <sub>2</sub>
C <sub>3</sub> H <sub>4</sub> O <sub>2</sub>	Propanedial	CHOCH <sub>2</sub> CHO
C <sub>2</sub> H <sub>2</sub> O <sub>2</sub>	Glyoxal	CHOCHO
C <sub>4</sub> H <sub>6</sub> O <sub>1</sub>	Butenal isomers	C <sub>3</sub> H <sub>5</sub> CHO
C <sub>3</sub> H <sub>4</sub> O <sub>1</sub>	Acrolein (propenal)	C <sub>2</sub> H <sub>3</sub> CHO
C <sub>6</sub> H <sub>10</sub> O <sub>1</sub>	Hexenal isomers	C <sub>5</sub> H <sub>9</sub> CHO

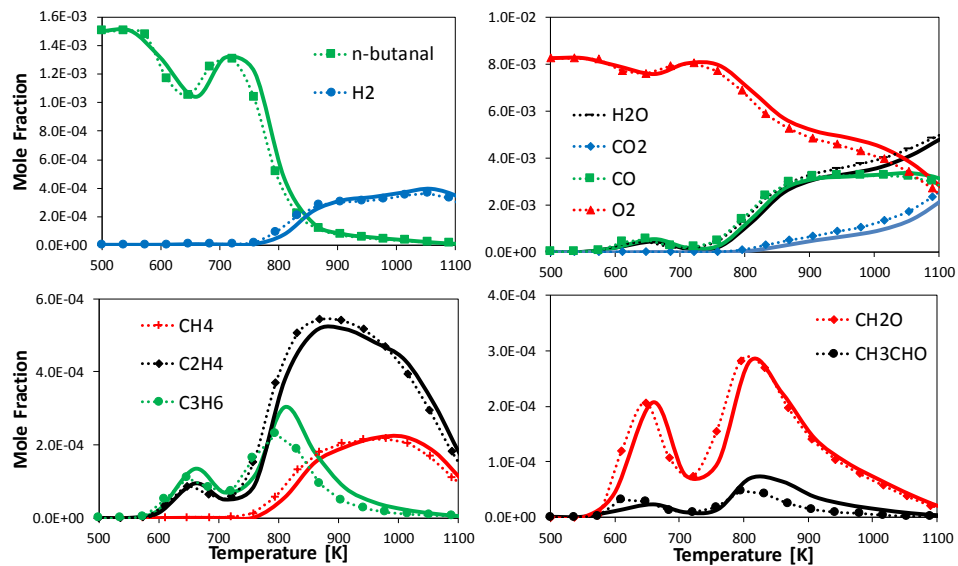


Figure S 22: Comparison between detailed n-butanal model (solid lines) (Pelucchi et al. Proceedings of the Combustion Institute 36.1 (2017): 393-401) and its lumped version (dashed lines with symbols). Conditions as in Figure S5.